Week 3
Lecture Notes:
Topological Condensed Matter Physics

Sebastian Huber and Titus Neupert

Department of Physics, ETH Zürich
Department of Physics, University of Zürich

If you notice mistakes or typos, please report them to michael.denner@physik.uzh.ch or periv@phys.ethz.ch

Chapter 3

One-dimensional topological phases

Learning goals

- We know the Su-Schrieffer-Herger model.
- We understand its bulk-boundary correspondence.
- We can characterize its topology through winding number invariants and Wilson loops.
- We understand the connection between Wilson loops, polarization, and the position operator.

- J. Zak, Phys. Rev. Lett. **62**, 2747–2750 (1989)
- L. Fidkowski, T. S. Jackson, and I. Klich, Phys. Rev. Lett. **107**, 036601 (2011)
- N. Marzari, A. A. Mostofi, J. R. Yates, I. Souza, and D. Vanderbilt, Rev. Mod. Phys. **84**, 1419 (2012)

In the following chapters, we are mostly concerned with the topological characterization of non-interacting electron Hamiltonians on a lattice. In general, an insulating topological phase of matter may be defined by the requirement that the many-body ground state of the corresponding Hamiltonian (given by a Slater determinant in the non-interacting case) cannot be adiabatically connected to the atomic limit of vanishing hopping between the sites of the lattice. Further requiring that certain symmetries such as time-reversal are not violated along any such adiabatic interpolation enriches the topological classification, in that phases which were classified as trivial in the previous sense now acquire a topological distinction which is protected by the respective symmetry.
In this chapter we will work towards an initial understanding of the fundamental topological properties of insulating (gapped) topological band structures. We will introduce topological invariants and the bulk-boundary correspondence. These concepts can be found in systems of any dimension and likewise we will introduce the bulk-boundary correspondence for arbitrary dimension, using a Wannier state approach. Specifically, we will learn how to employ Wilson loops as a generalization of the one-dimensional (1D) Berry phase to characterize topological properties of a phase. This provides a framework of topological invariants which makes direct contact with the protected boundary degrees of freedom of a given phase. As a pedagogical example for illustration, we will resort to the simplest case of one dimension and there specifically to the Su-Schrieffer-Heeger model throughout.

3.1 Definitions

In this chapter and the following ones, we will be concerned to a large extend with tight-binding models of non-interacting electron system. Therefore it is useful to clarify some notation first. We work in units where $\hbar = c = e = 1$ and denote by σ_i, $i = x, y, z$, the 2×2 Pauli matrices. We define $\sigma_0 = \mathbb{1}_{2\times 2}$ for convenience. We express eigenfunctions of a translationally invariant

single-particle Hamiltonian in the basis

$$\phi_{\boldsymbol{k},\alpha}(\boldsymbol{r}) = \frac{1}{\sqrt{N}} \sum_{\boldsymbol{R}} e^{\mathrm{i}\boldsymbol{k}\cdot(\boldsymbol{R}+\boldsymbol{r}_\alpha)} \varphi_{\boldsymbol{R},\alpha}(\boldsymbol{r}-\boldsymbol{R}-\boldsymbol{r}_\alpha), \tag{3.1.1}$$

where $\varphi_{\boldsymbol{R},\alpha}$, $\alpha = 1, \cdots, N$, are the orbitals chosen as basis for the finite-dimensional Hilbert space in each unit cell, labelled by the lattice vector $\boldsymbol{R}$, and $\boldsymbol{r}_\alpha$ is the center of each of these orbitals relative to the origin of the unit cell. Including $\boldsymbol{r}_\alpha$ in the exponential corresponds to a convenient choice of gauge when studying the response to external fields defined in continuous real space.
A general non-interacting Hamiltonian then has the Bloch matrix elements

$$\mathcal{H}_{\alpha,\beta}(\boldsymbol{k}) = \int \mathrm{d}^d r \phi^*_{\boldsymbol{k},\alpha}(\boldsymbol{r}) \hat{H} \phi_{\boldsymbol{k},\beta}(\boldsymbol{r}), \tag{3.1.2}$$

as well as energy eigenstates

$$\psi_{\boldsymbol{k},n}(\boldsymbol{r}) = \sum_{\alpha}^{N} u_{\boldsymbol{k};n,\alpha} \phi_{\boldsymbol{k},\alpha}(\boldsymbol{r}), \tag{3.1.3}$$

where

$$\sum_{\beta} \mathcal{H}_{\alpha,\beta}(\boldsymbol{k}) u_{\boldsymbol{k};n,\beta} = \epsilon_n(\boldsymbol{k}) u_{\boldsymbol{k};n,\alpha}, \qquad n = 1, \cdots, N. \tag{3.1.4}$$

In the following, we are interested in situations where the system has an energy gap after the first $M < N$ bands, i.e., $\epsilon_M(\boldsymbol{k}) < \epsilon_{M+1}(\boldsymbol{k})$ for all $\boldsymbol{k}$ in the first Brillouin zone (BZ).

3.2 The the Su-Schrieffer-Heeger model

One of the simplest examples of a topological phase is exemplified by the Su-Schrieffer-Heeger (SSH) model, initially devised to model polyacetylene. It describes electrons hopping on a 1D dimerized lattice with two sites A and B in its unit cell (see Fig 3.1***a***). In momentum space, the Bloch Hamiltonian reads

$$\mathcal{H}(k) = \begin{pmatrix} 0 & t + t' e^{\mathrm{i}k} \\ t + t' e^{-\mathrm{i}k} & 0 \end{pmatrix}. \tag{3.2.1}$$

The model has an inversion symmetry $I\mathcal{H}(k)I^{-1} = \mathcal{H}(-k)$, with $I = \sigma_x$. Since it does not couple sites A to A or B to B individually, it furthermore enjoys a chiral or sublattice symmetry $C\mathcal{H}(k)C^{-1} = -\mathcal{H}(k)$ with $C = \sigma_z$. [Notice some abuse of language here: The chiral symmetry is not a "symmetry" in the sense of a commuting operator on the level of the first quantized Bloch Hamiltonian. Still, as a mathematical fact, this chiral symmetry can be helpful to infer and protect the existence of topological boundary modes.] While a standard discussion of the SSH model would focus on the chiral symmetry and its role in protecting topological phases, here we will first consider the implications of the crystalline inversion symmetry. It will be useful to note that the spectrum is given by

$$\epsilon_\pm(k) = \pm\sqrt{t^2 + t'^2 + 2tt' \cos k} \tag{3.2.2}$$

with a gap closing at $k = \pi$ for $t = t'$ and at $k = 0$ for $t = -t'$. When $|t| \neq |t'|$, the system is thus insulating (gapped) and we can study its topological properties. The phases $t > t'$, $-t' < t < t'$, and $t < -t'$ are separated by gap closing and could thus potentially be topological different.

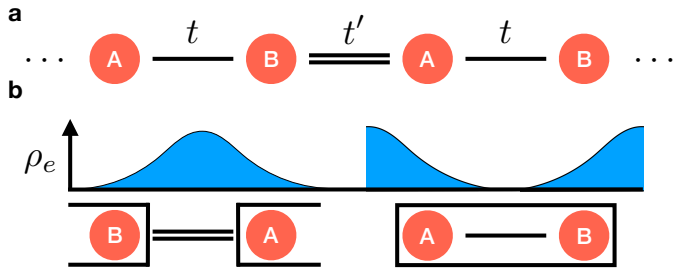

Figure 3.1: ***a*** The model consists of electrons hopping on a dimerized chain with alternating hopping strengths t and t'. For the case of $t' > t$, the model is in its topological phase, which is adiabatically connected to the special case $t' \neq 0$, $t = 0$. In this limit the presence of gapless edge modes is evident when the chain is cut after a full unit cell. ***b*** The polarization is a measure of where charges sit in the unit cell. Shown is the case $\mathsf{P} = 1/2$, where the charge center is displaced by exactly half a lattice spacing. When cutting the system after a full unit cell, the edge hosts a state of charge $1/2$. This is the simplest example of charge fractionalization in topological condensed matter systems.

3.3 Wilson loop and position operator

Introduced in 1984 by Sir Michael Berry, the so-called Berry phase describes a phase factor which arises in addition to the dynamical evolution $e^{\mathrm{i}\int E[\lambda(t)]dt}$ of a quantum mechanical state in an adiabatic interpolation of the corresponding Hamiltonian $H[\lambda(t)]$ along a closed path $\lambda(t)$ in parameter space. It depends only on the geometry of the path chosen, and can be expressed as a line integral of the Berry connection, which we define below for the case where the parameter λ is a single particle momentum. If degeneracies between energy levels are encountered along the path, we have to consider the joint evolution of a set of eigenstates that may have degeneracies. If we consider M such states, the Berry phase generalizes to a $U(M)$ matrix, which may be expressed as the line integral of a non-Abelian Berry connection, and is called non-Abelian Wilson loop.
In the BZ, we may consider momentum $\boldsymbol{k}$ as a parameter of the Bloch Hamiltonian $\mathcal{H}(\boldsymbol{k})$. The corresponding non-Abelian Berry-Wilczek-Zee connection is then given by

$$\boldsymbol{\mathcal{A}}_{m,n}(\boldsymbol{k}) = \langle u_{\boldsymbol{k},m} | \boldsymbol{\nabla}_{\boldsymbol{k}} | u_{\boldsymbol{k},n} \rangle, \qquad n, m = 1, \cdots, M. \tag{3.3.1}$$

Note that it is anti-Hermitian, that is, it satisfies $\boldsymbol{\mathcal{A}}^*_{n,m}(\boldsymbol{k}) = -\boldsymbol{\mathcal{A}}_{m,n}(\boldsymbol{k})$. Using matrix notation, we define the Wilson loop, a unitary operator, as

$$W[l] = \overline{\exp}\left[-\int_l \mathrm{d}\boldsymbol{l} \cdot \boldsymbol{\mathcal{A}}(\boldsymbol{k})\right], \tag{3.3.2}$$

where l is a loop in momentum space and the overline denotes path ordering of the exponential. This unitary operator acts on the occupied band manifold, and can be numerically evaluated

with the formula

$$
\begin{aligned}
W_{n_1,n_{R+1}}[l] &= \lim_{R\to\infty} \sum_{n_2,\cdots n_R=1}^{M} \prod_{i=1}^{R} \Big[\exp\left[-(\boldsymbol{k}_{i+1}-\boldsymbol{k}_i)\cdot\boldsymbol{\mathcal{A}}(\boldsymbol{k}_{i+1})\right]\Big]_{n_i,n_{i+1}} \\
&= \lim_{R\to\infty} \sum_{n_2,\cdots n_R=1}^{M} \prod_{i=1}^{R} \Big[\delta_{n_i,n_{i+1}} - (\boldsymbol{k}_{i+1}-\boldsymbol{k}_i)\cdot\boldsymbol{\mathcal{A}}_{n_i,n_{i+1}}(\boldsymbol{k}_{i+1})\Big] \\
&= \lim_{R\to\infty} \sum_{n_2,\cdots n_R=1}^{M} \prod_{i=1}^{R} \Big[\langle u_{\boldsymbol{k}_{i+1},n_i}|u_{\boldsymbol{k}_{i+1},n_{i+1}}\rangle \\
&\quad -(\boldsymbol{k}_{i+1}-\boldsymbol{k}_i)\cdot\langle u_{\boldsymbol{k}_{i+1},n_i}|\boldsymbol{\nabla}_{\boldsymbol{k}_{i+1}}|u_{\boldsymbol{k}_{i+1},n_{i+1}}\rangle\Big] \qquad (3.3.3) \\
&= \lim_{R\to\infty} \sum_{n_2,\cdots n_R=1}^{M} \prod_{i=1}^{R} \langle u_{\boldsymbol{k}_{i+1},n_i}|u_{\boldsymbol{k}_i,n_{i+1}}\rangle \\
&= \langle u_{\boldsymbol{k}_{R+1},n_1}| \lim_{R\to\infty} \prod_{i=2}^{R} \left(\sum_{n_i}^{M} |u_{\boldsymbol{k}_i,n_i}\rangle\langle u_{\boldsymbol{k}_i,n_i}|\right) |u_{\boldsymbol{k}_1,n_{R+1}}\rangle\,, \qquad (3.3.4)
\end{aligned}
$$

where the path l is sampled into R momenta $\boldsymbol{k}_i$, $i = 1,\cdots,R$, and the limit $R\to\infty$ is taken such that the distance between any two neighboring momentum points goes to zero. Further, $\boldsymbol{k}_1 = \boldsymbol{k}_{R+1}$ are the initial and final momenta along the loop, respectively, on which the Wilson loop matrix depends.

By the last line of Eq. (3.3.3) it becomes clear that $W[l]$ is gauge *covariant*, that is, transforms as an operator under a general gauge transformation $S(\boldsymbol{k}) \in U(M)$ of the occupied subspace given by $|u_{\boldsymbol{k}}\rangle \to S(\boldsymbol{k})\,|u_{\boldsymbol{k}}\rangle$, only for a closed loop l (the case where l is non-contractible is also referred to as the Zak phase). However, the Wilson loop *spectrum* for a closed loop is gauge *invariant*, that is, the eigenvalues of $W[l]$ are not affected by gauge transformations (note that they also do not depend on the choice of $\boldsymbol{k}_i = \boldsymbol{k}_f$) and may therefore carry physical information. We will show in the following that this is indeed the case: the Wilson loop spectrum is related to the spectrum of the position operator projected into the space of occupied bands.

To proceed, we consider a geometry where l is parallel to the x coordinate axis, and winds once around the BZ. Let $\boldsymbol{k}$ denote the $(d-1)$ dimensional vector of remaining good momentum quantum numbers. Then $W(\boldsymbol{k})$ is labelled by these remaining momenta. Denote by $\exp(\mathrm{i}\vartheta_{\alpha,\boldsymbol{k}})$, $\alpha = 1,\cdots,M$, the eigenvalues of $W(\boldsymbol{k})$. The set of phases $\{\vartheta_{\alpha,\boldsymbol{k}}\}$ forms a band structure in the $(d-1)$ dimensional BZ and is often equivalently referred to as the Wilson loop spectrum. Note that all $\vartheta_{\alpha,\boldsymbol{k}}$ are only defined modulo 2π, which makes the Wilson loop spectrum inherently different from the spectrum of a physical Bloch Hamiltonian.

The spectral equivalence we will show relates the eigenvalues of the operator $(-\mathrm{i}/2\pi)\log[W(\boldsymbol{k})]$ with those of the projected position operator

$$P(\boldsymbol{k})\hat{x}P(\boldsymbol{k}), \qquad (3.3.5)$$

where the projector $P(\boldsymbol{k})$ onto all occupied band eigenstates along l (i.e., all states with wave vector $\boldsymbol{k}$) is given by

$$P(\boldsymbol{k}) = \sum_{n}^{M} \int_{-\pi}^{\pi} \frac{\mathrm{d}k_x}{2\pi} |\psi_{\boldsymbol{k},n}\rangle\langle\psi_{\boldsymbol{k},n}|, \qquad (3.3.6)$$

where the states $|\psi_{\boldsymbol{k},n}\rangle$ are given by Eq. (3.1.3). The eigenvalues of the projected position operator have the interpretation of the charge centers in the ground state of the Hamiltonian considered, while the eigenstates are known as hybrid Wannier states, which are localized in the x-direction and plane waves perpendicular to it.

To prove the equivalence, we start with the eigenfunctions of $P(\boldsymbol{k})\hat{x}P(\boldsymbol{k})$, which satisfy

$$\left[P(\boldsymbol{k})\hat{x}P(\boldsymbol{k}) - \frac{\tilde{\vartheta}_{\boldsymbol{k}}}{2\pi}\right]|\Psi_{\boldsymbol{k}}\rangle = 0. \tag{3.3.7}$$

Note that there are M eigenvectors, the form of the corresponding eigenvalues $\tilde{\vartheta}_{\alpha,\boldsymbol{k}}/(2\pi)$, $\alpha = 1,\cdots,M$ has been chosen for later convenience and in particular has not yet been logically connected to the $\vartheta_{\alpha,\boldsymbol{k}}$ making up the Wilson loop spectrum (however, we will do so shortly). An eigenfunction can be expanded as

$$|\Psi_{\boldsymbol{k}}\rangle = \sum_n^M \int \mathrm{d}k_x\, f_{\boldsymbol{k},n}(k_x)|\psi_{\boldsymbol{k},n}\rangle, \tag{3.3.8}$$

where the coefficients $f_{\boldsymbol{k},n}$ satisfy the equation

$$\begin{aligned}
&\langle\psi_{\boldsymbol{k},n}|P(\boldsymbol{k})\hat{x}P(\boldsymbol{k})|\Psi_{\boldsymbol{k}}\rangle \\
=\;& \sum_m \int \mathrm{d}\tilde{k}_x\, \langle\psi_{\boldsymbol{k},n}|(\mathrm{i}\partial_{\tilde{k}_x})f_{\boldsymbol{k},m}(\tilde{k}_x)|\psi_{\tilde{\boldsymbol{k}},m}\rangle \\
=\;& \sum_m \int \mathrm{d}\tilde{k}_x\, \mathrm{i}\frac{\partial f_{\boldsymbol{k},m}(\tilde{k}_x)}{\partial\tilde{k}_x}(\delta_{m,n}\delta_{\tilde{k}_x,k_x}) \\
&+\sum_m \int \mathrm{d}\tilde{k}_x f_{\boldsymbol{k},m}(\tilde{k}_x)\int\frac{\mathrm{d}x}{2\pi}\left\langle u_{\boldsymbol{k},n}\left|e^{-\mathrm{i}k_x x}(\mathrm{i}\partial_{\tilde{k}_x})e^{\mathrm{i}\tilde{k}_x x}\right|u_{\tilde{\boldsymbol{k}},m}\right\rangle \\
=\;& \mathrm{i}\frac{\partial f_{\boldsymbol{k},n}(k_x)}{\partial k_x} - f_{\boldsymbol{k},n}(k_x)\int\frac{\mathrm{d}x}{2\pi}x + \mathrm{i}\sum_m\int\mathrm{d}\tilde{k}_x f_{\boldsymbol{k},m}(\tilde{k}_x)\int\frac{\mathrm{d}x}{2\pi}e^{-\mathrm{i}(k_x-\tilde{k}_x)x}\langle u_{\boldsymbol{k},n}|\partial_{k_x}|u_{\tilde{\boldsymbol{k}},m}\rangle \\
=\;& \mathrm{i}\frac{\partial f_{\boldsymbol{k},n}(k_x)}{\partial k_x} + \mathrm{i}\sum_m f_{\boldsymbol{k},m}(k_x)\langle u_{\boldsymbol{k},n}|\partial_{k_x}|u_{\boldsymbol{k},m}\rangle \\
=\;& \mathrm{i}\frac{\partial f_{\boldsymbol{k},n}(k_x)}{\partial k_x} + \mathrm{i}\sum_m^M \mathcal{A}_{x;n,m}(\boldsymbol{k})f_{\boldsymbol{k},m}(k_x).
\end{aligned} \tag{3.3.9, 3.3.10}$$

(Note that we have to assume an appropriate regularization to make the term $\int \mathrm{d}x\, x$ vanish in this continuum calculation, reflecting the ambiguity in choosing the origin of the coordinate system.) Then, integrating the resulting Eq. (3.3.7) for $f_{\boldsymbol{k},n}(k_x)$, we obtain

$$f_{\boldsymbol{k},n}(k_x) = e^{-\mathrm{i}(k_x-k_x^0)\tilde{\vartheta}_{\boldsymbol{k}}/(2\pi)}\sum_m^M \overline{\exp}\left[-\int_{k_x^0}^{k_x}\mathrm{d}\tilde{k}_x\mathcal{A}_x(\tilde{k}_x,\boldsymbol{k})\right]_{n,m} f_{\boldsymbol{k},m}(k_x^0). \tag{3.3.11}$$

We now choose $k_x = k_x^0 + 2\pi$. Periodicity of $f_{\boldsymbol{k},m}(k_x^0)$ as $k_x^0 \to k_x^0 + 2\pi$ yields (choosing $k_x^0 = \pi$ without loss of generality)

$$\sum_m^M W(\boldsymbol{k})_{n,m}f_{\boldsymbol{k},m}(\pi) = e^{\mathrm{i}\tilde{\vartheta}_{\boldsymbol{k}}}f_{\boldsymbol{k},n}(\pi), \tag{3.3.12}$$

showing that the expansion coefficients of an eigenstate of $P(\boldsymbol{k})\hat{x}P(\boldsymbol{k})$ with eigenvalue $\tilde{\vartheta}_{\boldsymbol{k}}/(2\pi)$ form eigenvectors of $W(\boldsymbol{k})$ with eigenvalues $e^{\mathrm{i}\tilde{\vartheta}_{\boldsymbol{k}}}$. This establishes the spectral equivalence $\tilde{\vartheta}_{\boldsymbol{k}} = \vartheta_{\boldsymbol{k}}$.

Note that there are M eigenvalues of the Wilson loop, while the number of eigenvalues of $P(\boldsymbol{k})\hat{x}P(\boldsymbol{k})$ is extensive in the system size. Indeed, for each occupied band (i.e., every Wilson loop eigenvalue $\vartheta_{\alpha,\boldsymbol{k}}$, $\alpha = 1,\cdots,M$) there exists a ladder of eigenvalues of the projected position operator

$$\frac{\vartheta_{\alpha,\boldsymbol{k},X}}{2\pi} = \frac{\vartheta_{\alpha,\boldsymbol{k}}}{2\pi} + X, \qquad X\in\mathbb{Z}, \qquad \alpha = 1,\cdots,M. \tag{3.3.13}$$

Notice that we have set the lattice spacing in the x-direction to 1 for convenience here and in the following.
The eigenstates of the projected position operator are then given by

$$\Psi_{\alpha,\boldsymbol{k}}(x-X)=\sum_{n}^{M}\int\frac{\mathrm{d}k_x}{2\pi}e^{-\mathrm{i}\left[\vartheta_{\alpha,\boldsymbol{k}}/(2\pi)+X\right]}f_{\boldsymbol{k},n;\alpha}(k_x)\psi_{\boldsymbol{k},n}(x), \tag{3.3.14}$$

i.e., they are hybrid Wannier states which are maximally localized in x direction, but take on plane wave form in the perpendicular directions. Note that since the eigenvalues of $W(\boldsymbol{k})$ along any non-contractible loop of $\boldsymbol{k}$ in the BZ define a map $S^1\to U(1)\cong S^1$, their winding number, which is necessarily an integer, provides a topological invariant that cannot be changed by smooth deformations of the system's Hamiltonian.

3.4 Wilson loops, polarization and the winding number invariant in the Su-Schrieffer-Heeger model

So far, this has been a rather formal and general introduction to Wilson loops and their connection to the projected position operator. To illustrate them, we go back to the example of the SSH model. Let us start by calculating the Wilson loop for the case where $(t,t')=(0,1)$. The eigenvectors of $\mathcal{H}(k)$ are then given by

$$|u_{k,1}\rangle=\frac{1}{\sqrt{2}}\begin{pmatrix}-e^{\mathrm{i}k}\\1\end{pmatrix},\quad |u_{k,2}\rangle=\frac{1}{\sqrt{2}}\begin{pmatrix}e^{\mathrm{i}k}\\1\end{pmatrix}, \tag{3.4.1}$$

with energies -1 and $+1$, respectively. Since the occupied subspace is one-dimensional in this case, the Berry connection $A(k)=\langle u_{k,1}|\partial_k|u_{k,1}\rangle=\mathrm{i}/2$ is Abelian and given by just a purely imaginary number (remember that it is anti-Hermitian in general). We thus obtain

$$\mathsf{P}:=-\frac{\mathrm{i}}{2\pi}\log W=-\frac{\mathrm{i}}{2\pi}\int_0^{2\pi}\mathcal{A}(k)\mathrm{d}k=\frac{1}{2}. \tag{3.4.2}$$

The physical interpretation of P is given within the modern theory of polarization as that of a bulk electrical dipole moment or charge polarization, which is naturally only defined modulo 1 since the coordinate of a center of charge on the lattice is only defined up to a lattice translation (remember that we have chosen the lattice spacing $a=1$). It is directly connected to the Wilson loop spectrum $\vartheta_{\alpha,\boldsymbol{k}}$ by a rescaling which makes sure that the periodicity of the charge centers defined in this way is that of the real-space lattice. See also Fig. 3.1***b***.
The result $\mathsf{P}=1/2$ is by no means accidental: In fact, since the inversion symmetry reverses the path of integration in W, but leaves inner products such as $A(k)$ invariant, the Wilson loop eigenvalues of an inversion symmetric system come in complex conjugate pairs, i.e., for each eigenvalue ϑ there exists another eigenvalue ϑ' such that $e^{\mathrm{i}\vartheta}=e^{-\mathrm{i}\vartheta'}$. In the Abelian case of a single band, this means that P be quantized to 0 ($\vartheta=0$) or $1/2$ ($\vartheta=\pi$). This is an example where a crystalline symmetry such as inversion, which acts non-locally in space, protects a topological phase by enforcing the quantization of a topological invariant to values that cannot be mapped into one another by an adiabatic evolution of the corresponding Hamiltonian. Note that since the eigenstates for the parameter choice $(t,t')=(1,0)$ do not depend on k, we immediately obtain $\mathsf{P}=0$ for this topologically trivial case.
By these considerations it is clear that in fact the full parameter regime where $t<t'$ is topological, while the regime $t>t'$ is trivial. This is because it is possible to perform an adiabatic interpolation from the specific parameter choices $(t,t')\in\{(0,1),(1,0)\}$ considered above to all other values as long as there is no gap closing and no breaking of inversion symmetry, which is true provided that the line $t=t'$ is avoided in parameter space.

In many cases, a topological phase comes with topologically protected gapless boundary modes on boundaries which preserve the protecting symmetry. For inversion symmetry, however, there are no boundaries satisfying this requirement. Even though the model at $(t, t') = (0, 1)$ has zero-mode end states [since in this case, $\mathcal{H}(k)$ does not act at all on the A (B) site in the unit cell at the left (right) edge of the sample], these modes can be removed from zero energy by generic local perturbations even without a bulk gap closing. To protect the end modes, we need to invoke the chiral symmetry, which implies that an eigenstate at any energy E is paired up with an eigenstate at energy $-E$. Eigenstates of the chiral symmetry can then only appear at $E = 0$. A spatially and spectrally isolated boundary mode at $E = 0$ can thus not be removed by perturbations that retain the chiral symmetry.
In fact, in the presence of chiral symmetry, the above discussion can be generalized to arbitrary one-dimensional models. In the eigenbasis of C, we can write any Hamiltonian with chiral symmetry in the form

$$\mathcal{H}(k) = \begin{pmatrix} 0 & q(k) \\ q^\dagger(k) & 0 \end{pmatrix}, \tag{3.4.3}$$

where for the SSH model the matrix $q(k)$ was given by just a complex number. The chiral symmetry allows for the definition of a winding number

$$\nu = \frac{\mathrm{i}}{2\pi} \int \mathrm{d}k \, \mathrm{Tr} \left[q(k) \partial_k q^\dagger(k) \right] \in \mathbb{Z}. \tag{3.4.4}$$

This winding number is a topological invariant, i.e., a quantized number that is the same in the entire phase. Note that the formulation of Eq. (3.4.4) is only possible when chiral symmetry is present. We can make contact with the overarching concept of Wilson loops by calculating the connection

$$\mathcal{A} = \frac{1}{2} q(k) \partial_k q^\dagger(k). \tag{3.4.5}$$

Thus the Wilson loop eigenvalues $e^{\mathrm{i}\vartheta_\alpha}$ satisfy

$$\frac{1}{2\pi} \sum_\alpha \vartheta_\alpha = \frac{\nu}{2} \bmod 1. \tag{3.4.6}$$

In particular, in the Abelian case, chiral symmetry thus implies the quantization of P to half-integer values, just as inversion symmetry did it above. An important distinction to be made is that with inversion symmetry, we have a $\mathbb{Z}_2$ topological classification (P can be either 0 or 1/2), while with chiral symmetry the winding number allows for a $\mathbb{Z}$ classification.

3.5 Bulk-boundary correspondence

As already mentioned, Wilson loops not only provide a convenient formulation of many topological invariants, but are also in one-to-one correspondence with the boundary degrees of freedom of the system considered. We will now show that indeed the spectrum of a Hamiltonian in the presence of a boundary is smoothly connected to the spectrum of its Wilson loop along the direction perpendicular to the boundary. Note that since the Wilson loop is determined entirely by the bulk Bloch Hamiltonian, this relation provides an explicit realization of the bulk-boundary correspondence underlying topological phases.
We consider a semi-infinite slab geometry with a single edge of the system at $x = 0$, while keeping $\boldsymbol{k}$ as good quantum numbers. From a topological viewpoint, the actual energetics of the band structure are irrelevant, and we can always deform the Hamiltonian for the sake of clarity to a spectrally flattened Hamiltonian where all bands above and below the gap are at energy $+1$ and -1, respectively, without closing the gap. It is therefore enough to work with

$$\mathcal{H}_{\mathrm{flat}}(\boldsymbol{k}) = 1 - 2P(\boldsymbol{k}) \tag{3.5.1}$$

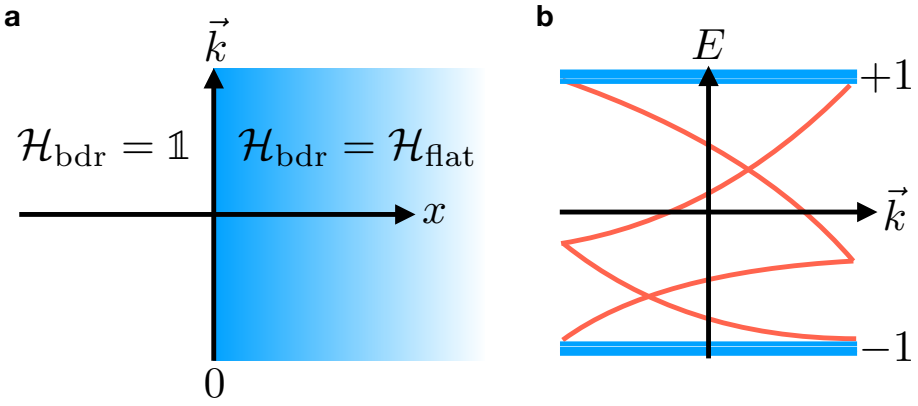

Figure 3.2: ***a*** For $V_0(x)$ as given by Eq. (3.5.4), $\mathcal{H}_{\rm bdr}$ varies discontinuously from a trivial projector in the domain $x < 0$ to $\mathcal{H}_{\rm flat}$ in the domain $x > 0$. Translational symmetry along x is thus broken, however it is preserved along all perpendicular directions, which still have good momentum quantum numbers $\boldsymbol{k}$. ***b*** The spectrum of $\mathcal{H}_{\rm bdr}$ has accumulation points at ± 1, stemming from the semi-infinite regions to the left and right of the domain wall, and a discrete set of bands in between, coming from the finite domain wall region.

to model the bulk system. Here, $P(\boldsymbol{k})$ as defined in Eq. (3.3.6), repeated here for convenience,

$$P(\boldsymbol{k}) = \sum_n^M \int_{-\pi}^{\pi} \frac{\mathrm{d}k_x}{2\pi} |\psi_{\boldsymbol{k},n}\rangle\langle\psi_{\boldsymbol{k},n}|, \tag{3.5.2}$$

is the projector onto the occupied subspace for a given $\boldsymbol{k}$. Note that $\mathcal{H}_{\rm flat}(\boldsymbol{k})$ actually has the same eigenvectors as the original Hamiltonian. To model a system with boundary, we use

$$\mathcal{H}_{\rm bdr}(\boldsymbol{k}) = P(\boldsymbol{k})V_0(\hat{x})P(\boldsymbol{k}) + 1 - P(\boldsymbol{k}), \tag{3.5.3}$$

with

$$V_0(x) = \begin{cases} 1 & x < 0 \\ -1 & x > 0 \end{cases} \tag{3.5.4}$$

so that we have $\mathcal{H}_{\rm bdr}(\boldsymbol{k}) \to \mathcal{H}_{\rm flat}(\boldsymbol{k})$ for $x \to +\infty$ and $\mathcal{H}_{\rm bdr}(\boldsymbol{k}) \to 1$ for $x \to -\infty$ (see Fig. 3.2***a***). The latter limit corresponds to a description of the vacuum with the chemical potential chosen so that no electron states will be occupied, which we take to be the topologically trivial limit. Since we take space to be infinitely extended away from the domain wall at $x = 0$, the spectrum of $\mathcal{H}_{\rm bdr}(\boldsymbol{k})$ includes the spectrum of $\mathcal{H}_{\rm flat}(\boldsymbol{k})$, given by ± 1 since $P^2(\boldsymbol{k}) = P(\boldsymbol{k})$, as well as that of the operator 1, trivially given by $+1$. The boundary region is of finite extent and can therefore contribute only a finite number of midgap states as the system has exponentially decaying correlations on either side of the boundary. There are therefore spectral accumulation points at ± 1, but otherwise we are left with a discrete spectrum (see Fig. 3.2***b***). We will focus on this part of the spectrum.

We will now deform the spectrum of $\mathcal{H}_{\rm bdr}(\boldsymbol{k})$ to that of $(-\mathrm{i}/2\pi)\log[W(\boldsymbol{k})]$ by considering an evolution that takes $P(\boldsymbol{k})V_0(\hat{x})P(\boldsymbol{k})$ to $P(\boldsymbol{k})\hat{x}P(\boldsymbol{k})$, the eigenvalues of which were previously shown to be directly related to those of $(-\mathrm{i}/2\pi)\log[W(\boldsymbol{k})]$. The deformation is continuous in $\boldsymbol{k}$ and therefore preserves both discreteness of the spectrum as well as its topological properties. An example for this interpolation is given by

$$V_\lambda(x) = \begin{cases} -\frac{x}{\lambda} & \text{for } |x| < \lambda/(1-\lambda) \\ -\frac{\mathrm{sgn}(x)}{1-\lambda} & \text{for } |x| \geq \lambda/(1-\lambda) \end{cases}, \qquad 0 \leq \lambda \leq 1. \tag{3.5.5}$$

Importantly, for any $\lambda < 1$, $P(\boldsymbol{k})V_\lambda(\hat{x})P(\boldsymbol{k})$ is a finite rank (finite support) perturbation of $(1-\lambda)^{-1}P(\boldsymbol{k})V_0(\hat{x})P(\boldsymbol{k})$, so it will retain the property that the spectrum is discrete. However, the point $\lambda = 1$ deserves closer inspection, as $P(\boldsymbol{k})\hat{x}P(\boldsymbol{k})$ is not a bounded operator. However, we can handle this subtlety by defining

$$h(r) = \begin{cases} r & \text{for } -w < r < w \\ \mathrm{sgn}(r)w & \text{else} \end{cases} \tag{3.5.6}$$

and considering $h[P(\boldsymbol{k})V_\lambda(\hat{x})P(\boldsymbol{k})]$ for some large w. The spectrum evolves uniformly continuously from $h[P(\boldsymbol{k})V_0(\hat{x})P(\boldsymbol{k})]$ to $h[P(\boldsymbol{k})V_1(\hat{x})P(\boldsymbol{k})]$ for any finite w.
The topology of the Wilson loop spectrum and the physical boundary spectrum is thus identical. Protected spectral flow in the former implies gapless boundary modes in the latter, as long as the form of the boundary [i.e., $V(x)$] does not break a symmetry that protects the bulk spectral flow.

References

1. Zak, J. "Berry's phase for energy bands in solids". *Phys. Rev. Lett.* **62,** 2747. https://doi.org/10.1103/PhysRevLett.62.2747 (1989).
2. Fidkowski, L., Jackson, T. & Klich, I. "Model Characterization of Gapless Edge Modes of Topological Insulators Using Intermediate Brillouin-Zone Functions". *Phys. Rev. Lett.* **107,** 036601. https://doi.org/10.1103/PhysRevLett.107.036601 (2011).
3. Marzari, N., Mostofi, A., Yates, J., Souza, I. & Vanderbilt, D. "Maximally localized Wannier functions: Theory and applications". *Rev. Mod. Phys.* **84,** 1419. https://doi.org/10.1103/RevModPhys.84.1419 (2012).